International Journal of Medical, Medicine and Health Sciences
ISSN: 2517-9969
Vol:5, No:12, 2011

Local Dynamic Mechanical Properties of Native Porcine Endplate

J. Sepitka, J. Lukes and J. Reznicek

***Abstract*—**Hysitron TriboIndenter™ TI 950 system has been used for studying the local viscoelastic properties of porcine intervertebral disc end plate by means of nanoscale mechanical dynamic analysis. The specimen of an endplate was cut from fresh porcine vertebra dissected from 16 month animal. The lumbar spine motion segments were dissected and 5 millimeter thick plates of vertebral body, endplate and annulus fibrosus were prepared for nanoindentation. The surface of the sample was kept in physiological solution during nanoindentation experiment. We obtained mechanical characteristics of different areas of native endplate (endplate middle and vertebra and annulus fibrosus boundary).

***Keywords*—**nanoindentation, DMA, endplate, cartilage

I. Introduction

LOW back pain is one of the major problem in Western industrialized societies. The number of people affected by pain varies between 15% and 35%. Low back pain causes an economic burden on society. Total losses caused by health care costs, by loss of production and by the reimbursement of sickness benefits in Great Britain estimated at 1.1% of gross domestic product and the Netherlands to 1.7% of gross domestic product [1].

Low back pain is closely related with intervertebral disc degeneration. Degeneration of intervertebral disc (IVD) is associated with nervus ischiaticus damage or with prolapsed disc. Degenerative changes of the IVD affect the mechanical behavior of the rest of the spine and thus can affect other spinal structures such as muscles and ligaments. These changes can point to spinal stenosis (narrowing of the spinal canal) in the longer time horizon, which is the main cause of back pain in elderly population [1].

The nutrition and removal of metabolic products depend largely on diffusion through the cartilaginous endplate (Fig. 1)because IVD does not contain blood vessels. Endplate is a layer of hyaline cartilage between the IVD and vertebral body [3]. The calcification of the endplate (Fig. 2) causes restriction of the IVD nutrition and its failure afterwards. The endplate also prevents a loss of a small proteoglycans from the IVJ and provides significant mechanical role of transferring loads between IVD and vertebral body.Information on mechanical properties from different parts of the endplate could help

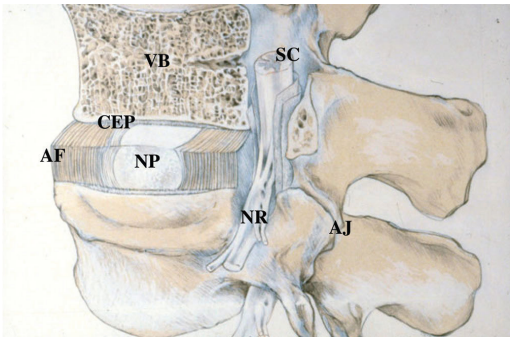

Fig. 1 A schematic view of a spinal segment and the intervertebral disc. The figure shows the organization of the disc with the nucleus pulposus (NP) surrounded by the lamellae of the annulus fibrosus (AF) and separated from the vertebral bodies (VB) by the cartilaginous end-plate (CEP). The figure also shows the relationship between the intervertebral disc and the spinal cord (SC), the nerve root (NR), and the apophyseal joints (AJ).Adopted from Urban et al. (2004) [4].

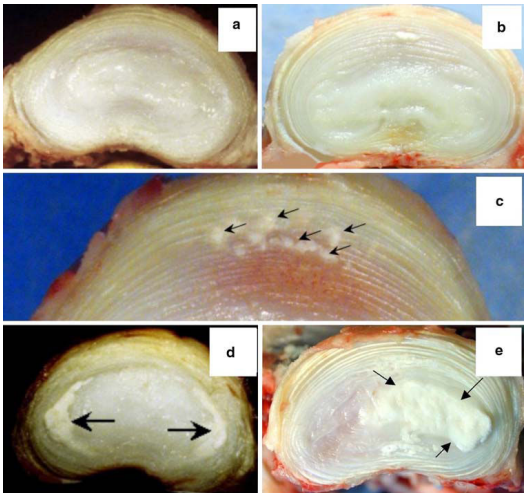

Fig. 2 Morphologic appearance of horizontally bisected ovine discs depicting no calcification in 2-ear-old L3L4 and 4-year-old L5L6 IVDs, respectively (a, b). Small punctate annular calcific deposits in the anterior annulus of L4L5 of 4-year-old (c); moderate calcification predominantly in the transitional zone of 4-year-old L3L4 IVD (d); heavy deposition of calcium in the TZ/NP L5L6 11-year-old IVD (e). Arrows depict the deposits. Adopted from Melrose et al (2009)[4]

J. Sepitka is with the Czech Technical University in Prague, Faculty of Mechanical Engineering, Dep. of Mechanics, Biomechanics and Mechatronics, Technická 4, 16607 Prague 6, Czech Republic (phone: +420-22435-2649; fax: +420-233-322-482 ; e-mail: Josef.Sepitka@fs.cvut.cz).

J. Lukes is with the Czech Technical University in Prague, Faculty of Mechanical Engineering, Dep. of Mechanics, Biomechanics and Mechatronics, Technická 4, 16607 Prague 6, Czech Republic (e-mail: Jaroslav.Lukes@fs.cvut.cz).

J. Reznicek is with the Czech Technical University in Prague, Faculty of Mechanical Engineering, Dep. of Mechanics, Biomechanics and Mechatronics, Technická 4, 16607 Prague 6, Czech Republic (e-mail:Jan.Reznicek@fs.cvut.cz).

with indentifying the causes of the failure of IVD.The aim of this work is to characterize the local mechanical viscoelastic characteristic of the native endplate using nanoindentation by dynamic mechanical analysis.

II. Materials and Methods

A. Sample preparation

A porcine cartilaginous endplate of lumbar spine L4 was used in our study. The specimen of endplate was cut from fresh porcine vertebra, dissected from 16 month animal. The lumbar spine motion segments were immediately dissected and five millimeter thick plates of vertebral body, end plate and annulus fibrosus were cut and polished under running water condition. Samples were placed into the physiological solution right after. Specimen was glued to the bottom of the Petri dish and surrounded by physiological solution again. The surface was under physiological solution and ready to be indented under a water level [8, 9].

B. Testing condition

Nanoscale dynamic mechanical analysis (nanoDMA) load controlled experiment was performed with Hysitron TriboIndenter^{TM} system with Berkovich diamond tip at the temperature 22.5 °C.Harmonic loading $P_0 = sin(\omega t)$ with dynamic load amplitude P_0 = 20 μN was specified for the harmonic frequency range 5-200 Hz. During nanoDMA experiment was applied static load with maximum force P_{max} = 800 μN. That corresponded to the contact indentation depth approximately h_c= 500 nm. Configuration of measurement was assumed from Lukeš et. al. (2010) [9]. The amplitude of the displacement oscillation X_0 and Φ the phase shift of the displacement with respect to the driving force are recorded by the nanoindentation system. The machine compliance C_i and the stiffness value K_i were determining during air indent calibration. The procedure was adopted from Asif et. al. (1999) [6] as well as the analysis of dynamic data.

C. Theory of nanoDMA

Dynamic driving force $P_0\sin(\omega t)$ with amplitude P_0 and frequency $f=\omega/2\pi$ is superimposed on quasistatic loading P_{max} and stands for particular term in an equation of motion of the indenter relative to the indenter head:

$$P_0 \sin(\omega t) = m\ddot{x} + C\dot{x} + Kx \tag{1}$$

The solution to the above equation, where compliance $C=C_i+C_s$ and stiffness $K=K_i+K_s$ of the system on Fig. 3 are defined respectively, is a steady-state displacement oscillation at the same frequency as the harmonic loading

$$x = X_0 \sin(\omega t - \phi) \tag{2}$$

where X_0 is the amplitude of the displacement oscillation and Φ is the phase shift of the displacement with respect to the driving force. Both terms in Eq. 2 are recorded by the nanoindentation system.

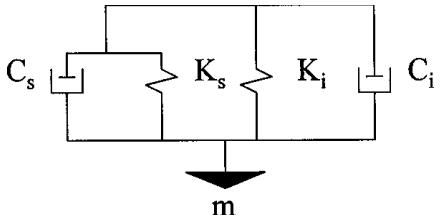

Fig. 3 Dynamic model of indenter system in contact with the specimen, where m is the indenter mass, C_i is the damping coefficient of the air gap in the capacitive displacement sensor, C_s is the damping coefficient of the specimen, K_s is the contact stiffness, and K_i is the spring constant of the leaf springs that hold the indenter shaft. Adopted from Asif et *al.* [6].

The standard analytical solution for the model on Fig. 3, that assumes that the machine frame stiffness K_i is infinite, follows.

The amplitude of the displacement signal is X_0 and the phase shift between force and displacement is Φ are given by

$$X_0 = \frac{P_0}{\sqrt{(K_s + K_i - m\omega^2)^2 + \left[(C_i + C_s)\omega\right]^2}} \tag{3}$$

$$\phi = \tan^{-1} \frac{(C_i + C_s)\omega}{K_s + K_i - m\omega^2} \tag{4}$$

where m is the indenter mass, ω is the frequency in rad/s, C_i is the damping coefficient of the air gap in the capacitive displacement sensor, C_s is the damping coefficient of the specimen, K_i is the spring constant of the leaf springs that hold the indenter shaft and K_s is the contact stiffness [6].

These calculated values for stiffness and damping of the sample are then used for determination of the viscoelastic properties of reduced storage modulus (E_r'), loss modulus (E_r'') and $tan\delta = E_r'/E_r''$.

$$E_r' = \frac{K_s\sqrt{\pi}}{2\sqrt{A_c}} \tag{5}$$

$$E_r'' = \frac{\omega C_s\sqrt{\pi}}{2\sqrt{A_c}} \tag{6}$$

$$\tan\delta = \frac{C_s\omega}{K_s} \tag{7}$$

where A_c is the contact area based on tip area function related to the contact depth at quasistatic loading [7]. The storage and loss modulus of the sample E_s' and E_s'', respectively, are related to the reduced storage and loss modulus by

$$\frac{1}{E_r'} = \frac{\left(1-\nu_i^2\right)}{E_i} + \frac{\left(1-\nu_s^2\right)}{E_s'} \tag{8}$$

$$\frac{1}{E_r''}=\frac{\left(1-\nu_i^2\right)}{E_i}+\frac{\left(1-\nu_s^2\right)}{E_s''} \quad (9)$$

where subscripts i and s refer to the indenter and sample materials, respectively, and ν is the Poisson's ratio.

The storage modulus and the loss modulus are related to the complex modulus $E_s^*=E_s'+iE_s''$ and indicate the ability of the sample to store and return energy (recoverable deformation; E_s') and dissipate energy (E_s''). The ratio of the loss modulus to the storage modulus (i.e., $tan\ \delta$) reflects the viscoelastic behavior of the material. It is a material parameter independent of the tip-sample contact area.

III. Results

Nanoscale dynamic mechanical analysis of different areas of native porcine intervertebral L4 disc endplate was performed. We tested three areas of the endplate which were different in vertical position, i. e. first one was very close to annulus fibrosus, second one was in the middle of the endplate and last one was very close to the vertebral body.Fig. 4-6 show measured nanoDMA characteristic of storage E_s' and loss moduli E_s'' vs. frequency. There were approximately the same average values of storage moduli at regions close to annulus fibrosus and in the middle of the endplate for initial frequency 5 Hz (Fig. 4, 5 and 7). There was monitored growth of the storage moduli for the sample at the margin of the endplate but not that rapid growth for middle zone of the endplate. There were measured lowest storage moduli very close to the bone tissue of vertebral body (Fig. 6). Loss moduli followed the same trends for all sample regions.

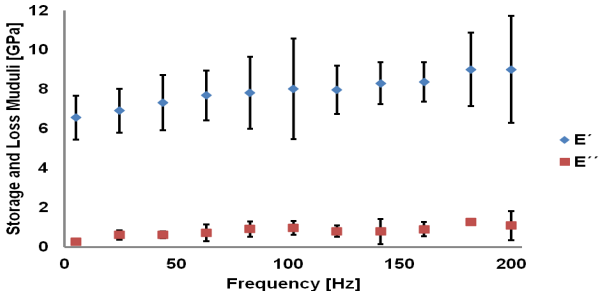

Fig. 4 Storage E' and loss E'' moduli from nanoDMA of porcine intervertebral L4 disc´s endplate measured very close to the annulus fibrosus.

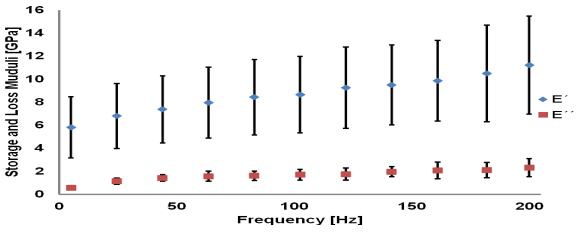

Fig. 5 Storage E' and loss E'' moduli from nanoDMA of porcine intervertebral L4 disc´s endplate measured in the middle of the endplate

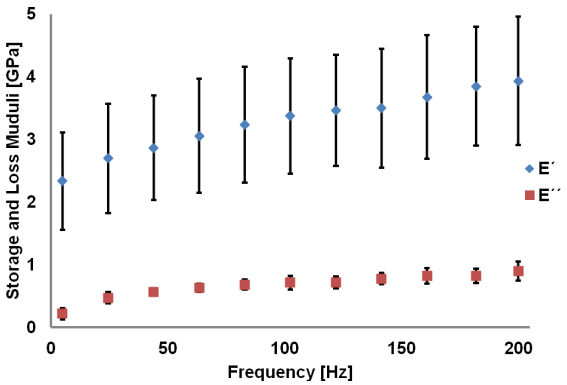

Fig. 6 Storage E' and loss E'' moduli from nanoDMA of porcine intervertebral L4 disc´s endplate measured very close to the bone body of the vertebra.

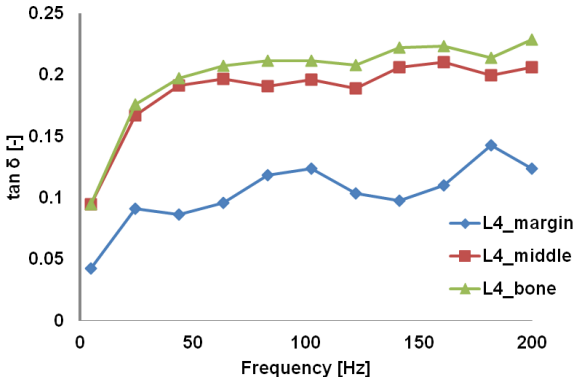

Fig. 7 Damping of all tested positions of the endplate couched in relation of $tan\ \delta$ and frequency.

IV. Conclusion

We expected an increasing gradient of moduli cartilaginous endplate being as a transition zone between very soft tissue of annulus fibrosus and hard tissue of vertebral body from marginal region to vertebral body. However, this hypothesis has not been confirmed at all. The highest stiffness and elastic behavior was observed at margin of AF and EP. More likely the local mechanical properties reflect inner structure of endplate, which is still a matter of scientific discussions. Some microstructural studies with finite element analysis needs to be correlated with mechanical responses representing by indentation curves. Nanoscale dynamic mechanical analysis was found to be a very good and sensitive method for an assessment of soft tissue mechanical testing

Acknowledgment

This work was supported by Ministry of Education project: Transdisciplinary research in Biomedical Engineering II. No. MSM 6840770012 and by the Grant Agency of the Czech Technical University in Prague, grant No. SGS10/247/OHK2/3T/12.

REFERENCES

[1] URBAN, Jill PG; ROBERTS, Sally. Degeneration of intervertebral disc. *Arthritis Research & Therapy*. 11 Mar 2003, No 3, s. 120-130.
[2] LOTZ, J. C., et al. Mechanobiology of the intervertebral disc. *Biomechanical Society*. 2002, 30, s. 853-858.
[3] ROBERTS, S.; MENAGE, J.; URBAN, J. P. G. Biochemical and Structural Properties of the Cartilage End-Plate and its Relation to the Intervertebral Disc. *Spine*. 1989, 2, s. 166-74.
[4] Melrose, J., D. Burkhardt, T. K. F. Taylor, C. T. Dillon, R. Read, M. Cake and C. B. Little, European Spine Journal, 18:479–489 (2009).
[5] BROCKBANK, Kelvin G. M., et al. Quantitative second harmonic generation imaging of cartilage damage. *Cell Tissue Banking*. 2008, 9, s. 299-307.
[6] Asif, S. A. S., Wahl, K. J., Colton, R. J.: Review of Scientific Instruments, 70, 5, 2408-2413 (1999).
[7] W. C., Pharr, G. M.: J. of Material Research, 7, 1564-1583 (1992).
[8] Sepitka, J., Lukes, Kuzelka, J., Reznicek, J.: Nanoscale dynamic mechanical analysis of soft tissue and its finite element modeling. *Chemické Listy*. DOPLNIT
[9] Lukes, J., Sepitka, J., Nemecek, J.: Dynamic nanoindentation of bovine intervertebral end plate; *Chemické Listy*.**104**, 15, p. 338-341 (2010).